



# Synthesis of 10 nm $\beta$ -NaYF<sub>4</sub>:Yb,Er/NaYF<sub>4</sub> Core/Shell Upconversion Nanocrystals with 5 nm Particle Cores

Thorben Rinkel, Athira Naduviledathu Raj, Simon Dühnen, and Markus Haase\*

**Abstract:** A new method is presented for preparing gram amounts of very small core/shell upconversion nanocrystals without additional codoping of the particles. First, ca. 5 nm  $\beta$ -NaYF<sub>4</sub>:Yb,Er core particles are formed by the reaction of sodium oleate, rare-earth oleate, and ammonium fluoride, thereby making use of the fact that a high ratio of sodium to rare-earth ions promotes the nucleation of a large number of  $\beta$ -phase seeds. Thereafter, a 2 nm thick NaYF<sub>4</sub> shell is formed by using 3–4 nm particles of  $\alpha$ -NaYF<sub>4</sub> as a single-source precursor for the  $\beta$ -phase shell material. In contrast to the core particles, however, these  $\alpha$ -phase particles are prepared with a low ratio of sodium to rare-earth ions, which efficiently suppresses an undesired nucleation of  $\beta$ -NaYF<sub>4</sub> particles during shell growth.

In recent years, numerous research papers have been published on the synthesis of upconversion nanocrystals for applications in biological labeling, sensing and imaging,<sup>[1–3]</sup> photodynamic therapy,<sup>[3]</sup> spectral conversion in solar cells,<sup>[1,4,11]</sup> 3D optical displays,<sup>[1]</sup> optical storage,<sup>[1,5]</sup> lasers,<sup>[6]</sup> and security printing.<sup>[1,7]</sup> The extensive literature on the synthesis, properties, and applications of NaREF<sub>4</sub> nanocrystals (RE = rare-earth) has already been summarized in several review articles.<sup>[1,2c,3b,c,4b,8]</sup> Solvent-dispersible NaREF<sub>4</sub> nanocrystals with controlled size, shape, and capping ligands have in fact been prepared by a variety of synthetic procedures, including thermal decomposition,<sup>[9]</sup> co-precipitation,<sup>[4a,10,11]</sup> and solvothermal methods.<sup>[2b,12]</sup> For biolabeling and imaging applications, however, nanocrystals with small size are preferred.<sup>[13]</sup> NaREF<sub>4</sub> nanocrystals with a mean size of about 5 nm and a narrow size distribution can in fact be synthesized for all rare-earth ions by heating sodium oleate, rare-earth oleate, and a fluoride source like NH<sub>4</sub>F in solutions containing oleic acid to 200–290 °C. This reaction yields particles of the more preferred hexagonal  $\beta$ -phase, however, only for rare-earth ions of group I (RE = La, Ce, Nd, Pr)<sup>[14]</sup> and group II (RE = Sm, Eu, Gd, Tb),<sup>[15]</sup> whereas the small particles obtained for group III elements (RE = Y, Ho, Er, Tm, Yb, Lu) usually consist of the cubic  $\alpha$ -phase. In the latter case, particles of the  $\beta$ -phase can be prepared by increasing the temperatures to 300–320 °C (in oleic acid containing solutions), but the size of the resulting particles is usually much larger than 5 nm. To reduce the size of NaYF<sub>4</sub>:Yb,Er upconversion particles, additional co-doping with group II

elements like gadolinium has been suggested by several groups.<sup>[16]</sup>

Until now, however, only two protocols exist for the preparation of nearly monodisperse 5 nm  $\beta$ -NaYF<sub>4</sub>:Yb,Er upconversion particles without additional doping.<sup>[11]</sup> In one of these methods the Na/Y ratio is varied to affect the nucleation of  $\beta$ -phase seeds.<sup>[11b]</sup> If a low ratio of sodium oleate to yttrium oleate is used in the synthesis of the  $\alpha$ -phase particles, heating at higher temperatures yields  $\beta$ -phase particles of large size, showing that only a small number of  $\beta$ -phase seeds were formed. When the Na/Y ratio is increased, however, the number of  $\beta$ -phase seeds also increases, leading to  $\beta$ -NaYF<sub>4</sub>:Yb,Er particles with smaller sizes down to 5 nm. Nanocrystals in this size regime, however, show high luminescence quantum yields only if a shell or a surface layer of a suitable material reduces luminescence quenching at the particle surface. In the case of  $\beta$ -NaYF<sub>4</sub>:Yb,Er upconversion particles, undoped NaYF<sub>4</sub> is the standard shell material for this purpose although other NaREF<sub>4</sub> materials have also been proposed.<sup>[9f,10a]</sup> The deposition of a NaREF<sub>4</sub> shell consisting of a group III element like yttrium, however, is complicated by the fact that  $\alpha$ -phase particles of the shell material are formed as the first product. Shell growth is then only possible at temperatures where these initially formed  $\alpha$ -phase particles dissolve again. Since the material thereby released must react with the surface of the core particles, the reaction conditions must be carefully chosen in order to avoid the nucleation of new  $\beta$ -phase particles of pure shell material. In the work presented here, this is achieved by using different ratios of sodium oleate to yttrium oleate in the synthesis of the core and the shell material. The  $\beta$ -NaYF<sub>4</sub>:Yb,Er core particles are synthesized with a high ratio of sodium to rare-earth ions resulting in nucleation of a large number of very small upconversion particles with a size of only ca. 5 nm. The small  $\alpha$ -NaYF<sub>4</sub> particles used as precursors for growing the NaYF<sub>4</sub> shell, however, are prepared with a low Na/Y ratio, in order to prevent the nucleation of new particles. Since the procedure involves neither the dropwise addition nor the rapid mixing of components at high temperature, rather large amounts of 10 nm core/shell upconversion particles with a core size of only ca. 5 nm can be prepared.

The  $\beta$ -NaYF<sub>4</sub>:Yb,Er core particles are prepared by heating sodium oleate, rare-earth oleate, and NH<sub>4</sub>F in a molar ratio of 8:1:11 in oleic acid/octadecene at 300 °C. The XRD data of samples drawn at different times of heating show that 3–4 nm particles of the cubic  $\alpha$ -phase are formed as an intermediate product (Figure 1). In contrast to our previously published procedure the intermediately formed NaYF<sub>4</sub>:Yb,Er particles of the cubic  $\alpha$ -phase were not isolated and redispersed in fresh solvent prior to conversion to the  $\beta$ -

[\*] T. Rinkel, A. N. Raj, S. Dühnen, Prof. Dr. M. Haase  
Institute of Chemistry of New Materials, University of Osnabrück  
Barbarastrasse 7, 49076 Osnabrück (Germany)  
E-mail: markus.haase@uni-osnabrueck.de

Supporting information for this article is available on the WWW under <http://dx.doi.org/10.1002/anie.201508838>.

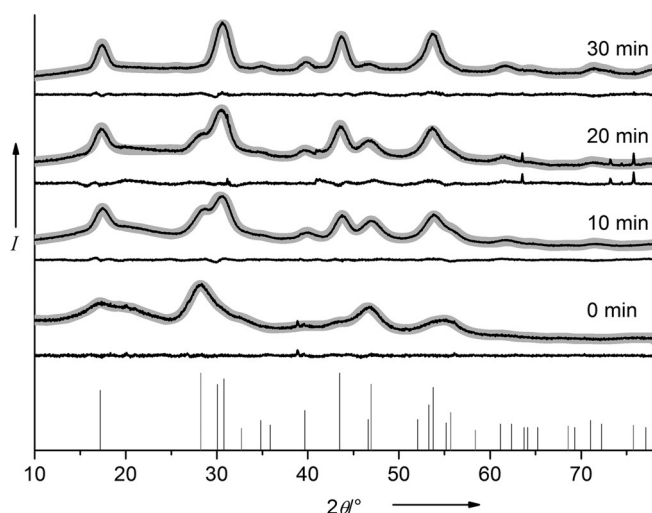


**Figure 1.** Formation of ca. 5 nm  $\beta$ -phase  $\text{NaYF}_4\text{:Yb,Er}$  nanoparticles at 300°C in oleic acid/octadecene by the reaction of sodium oleate, rare-earth oleate, and  $\text{NH}_4\text{F}$  in a molar ratio of 8:1:11. The chart displays the X-ray powder diffraction (XRD) data of samples drawn at different stages of the reaction at 300°C. Rietveld refinements of the data sets are included (solid lines). Small  $\text{NaYF}_4\text{:Yb,Er}$  particles of the cubic  $\alpha$ -phase are formed as the first product. Vertical lines correspond to the reference data of  $\text{NaYF}_4$ . Gray: cubic  $\alpha$ -phase, PDF No. 01-077-2042; black: hexagonal  $\beta$ -phase, PDF No. 00-016-0334.

phase. Nevertheless, both procedures yield  $\beta\text{-NaYF}_4\text{:Yb,Er}$  particles of the same small size of ca. 5 nm and in both cases the conversion to  $\beta$ -phase particles is completed within 40 minutes (Figure 1). When heating is stopped just after full conversion is achieved, the ca. 5 nm  $\beta\text{-NaYF}_4\text{:Yb,Er}$  particles retain their narrow size distribution as shown in the TEM image in Figure 2a (HRTEM images in Figure S1). The small size of the  $\beta$ -phase particles shows that a large number of  $\beta$ -phase seeds must have formed during the reaction.

A different growth dynamic is observed, however, when the 3–4 nm  $\alpha$ -phase particles are prepared with a molar ratio of 2:1:5 (sodium oleate/rare-earth oleates/ $\text{NH}_4\text{F}$ ). When these  $\alpha$ -phase particles are redispersed in new solvent and heated at 300°C, complete conversion to  $\beta\text{-NaYF}_4$  particles is observed, but the size of the final  $\beta$ -phase particles is 42 nm instead of ca. 5 nm (Figure 2c). This much larger particle size confirms our earlier studies showing that significantly fewer  $\beta$ -phase seeds are formed when the  $\alpha$ -phase precursor particles are prepared with a low molar ratio of sodium to rare-earth metal.<sup>[11b,17]</sup> Furthermore, the conversion to the  $\beta$ -phase proceeds much slower in this case. The latter is shown in Figure 3, which displays the fraction of  $\alpha$ -phase material present at different stages of heating at 300°C (black squares). The molar fractions of  $\alpha$ -phase and  $\beta$ -phase material were determined by removing samples from the reaction mixture, precipitating the nanocrystals, and performing a Rietveld analysis of their XRD data (see Figures S2–S4 in the Supporting Information). For comparison, Figure 3 also includes the conversion curve of redispersed  $\alpha$ -phase particles which are prepared with a molar ratio of 8:1:11 (black dots). The plot shows that the conversion of these particles to the  $\beta$ -phase is already completed before the conversion of  $\alpha$ -phase

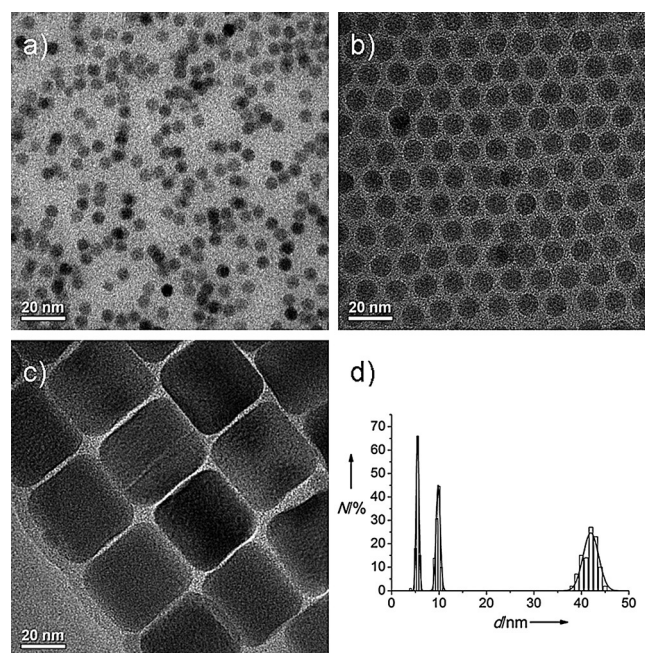


**Figure 2.** TEM images of a) ca. 5 nm  $\beta\text{-NaYF}_4\text{:Yb,Er}$  core particles, b) 10 nm  $\beta\text{-NaYF}_4\text{:Yb,Er}/\beta\text{-NaYF}_4$  core/shell particles, prepared from the ca. 5 nm core particles, and c) 42 nm  $\beta\text{-NaYF}_4$  particles obtained by heating the  $\alpha$ -phase  $\text{NaYF}_4$  precursor particles for the shell in the absence of core particles. d) Size histograms of (a), (b), and (c) showing standard deviations ( $\sigma/d$ ) of 5.5%, 4.5%, and 3.9%, respectively.

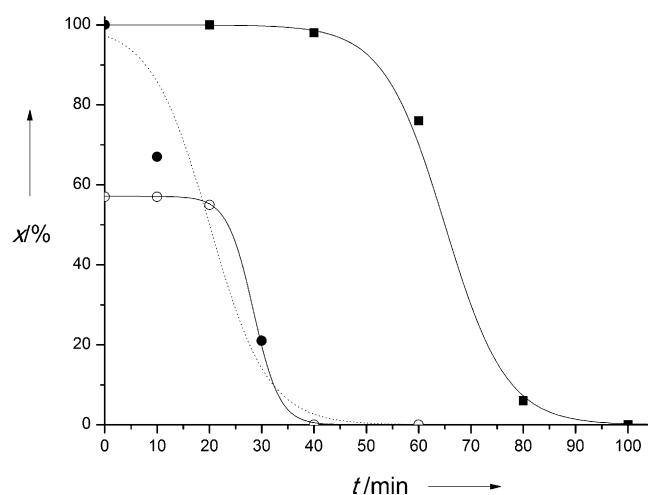


**Figure 3.** Conversion of  $\alpha$ -phase particles to  $\beta$ -phase particles during heating at 300°C in oleic acid/octadecene. The graphs show the molar fraction of  $\alpha$ -phase material remaining after different times of heating, as derived from XRD data. (●) Fast conversion of redispersed  $\alpha\text{-NaYF}_4\text{:Yb,Er}$  particles prepared with sodium oleate, rare-earth oleate, and  $\text{NH}_4\text{F}$  in a molar ratio of 8:1:11. (■) Delayed conversion of  $\alpha\text{-NaYF}_4$  particles prepared with a molar ratio of 2:1:5. (○) Fast conversion, when the  $\alpha\text{-NaYF}_4$  particles prepared with a molar ratio of 2:1:5 are heated in the presence of ca. 5 nm  $\beta\text{-NaYF}_4\text{:Yb,Er}$  core particles. This reaction yields core/shell particles.

particles prepared with a ratio of 2:1:5 has even started (black squares).

The key idea now is to use  $\alpha$ -phase particles prepared with a ratio of 2:1:5 as a single-source precursor for the shell, because they form undesired  $\beta$ -phase particles of pure shell material only after prolonged heating. The core/shell particles are thus prepared by synthesizing 3–4 nm  $\alpha$ -NaYF<sub>4</sub> particles with a molar ratio of 2:1:5, redispersing these particles together with ca. 5 nm  $\beta$ -NaYF<sub>4</sub>:Yb,Er core particles in new solvent and heating this colloidal mixture to 300 °C. Figure 3 shows that in the presence of the ca. 5 nm  $\beta$ -NaYF<sub>4</sub>:Yb,Er particles the molar fraction of  $\alpha$ -phase material decreases much faster than without them. The faster conversion to the  $\beta$ -phase indicates again that the  $\beta$ -phase particles act as seeds rapidly consuming the ions released by the dissolving  $\alpha$ -phase particles.<sup>[18]</sup> This is further confirmed by the final particle sizes obtained. The TEM images show that in the presence of the ca. 5 nm  $\beta$ -NaYF<sub>4</sub>:Yb,Er core particles (Figure 2a), the  $\alpha$ -NaYF<sub>4</sub> particles form particles with a mean size of ca. 10 nm instead of 42 nm (Figure 2b,c). Since the  $\beta$ -NaYF<sub>4</sub>:Yb,Er core and the  $\alpha$ -NaYF<sub>4</sub> shell material were used in a molar ratio of 1:3.5, the shell is expected to increase the volume of each core particle by a factor of 4.5 and their diameter by the cubic root of this factor, i.e., by  $4.5^{1/3} = 1.65$ . From the size histograms in Figure 2d, mean diameters  $\langle d \rangle$  and standard deviations ( $\sigma/\langle d \rangle$ ) of 5.5 nm  $\pm$  5.5 %, 9.8 nm  $\pm$  4.5 %, and 42 nm  $\pm$  3.9 % are calculated for the core particles, core/shell particles, and the larger particles of pure  $\beta$ -NaYF<sub>4</sub> shell material, respectively. The NaYF<sub>4</sub> shell should therefore increase the size of the NaYF<sub>4</sub>:Yb,Er core particles from 5.5 nm to  $5.5 \times 1.65$  nm = 9.1 nm, in good agreement with the measured value of 9.8 nm. Moreover, the size histograms and the TEM images show narrow size distributions in all cases, in accord with theory.<sup>[18]</sup> A schematic drawing of the formation of the core/shell particles is given in Figure S5 in the Supporting Information as well as additional overview TEM images used for the histograms (Figure S6).

Upon excitation at 978 nm, the Yb,Er-doped samples display the characteristic two-photon upconversion emission in the green and red spectral region along with some weak emission in the blue caused by the corresponding three-photon process (Figure S7). In Figure 4, the upconversion intensities of our samples are compared with the emission of bulk material, i.e., microcrystalline  $\beta$ -NaYF<sub>4</sub>:Yb,Er UC phosphor powder. Within our range of excitation densities, double-logarithmic plots of the combined intensity of the red and green emissions versus the excitation density yields straight lines with a slope of 2 for all samples. Similar to results published by other groups,<sup>[9d–f,11a,19]</sup> the upconversion intensity of NaYF<sub>4</sub>:Yb,Er nanoparticles strongly depends on the particle size and the core/shell structure. As expected, the lowest upconversion efficiency is observed for the ca. 5 nm NaYF<sub>4</sub>:Yb,Er core particles, because of their large surface-to-bulk ratio. Smaller particles require a smaller number of energy transfer steps between adjacent dopant ions to reach the surface where radiationless deactivation of the excitation energy is likely to take place. Moreover, a higher fraction of erbium ions is located at surface sites where their emission is easily quenched. The ca. 5 nm core particles therefore show

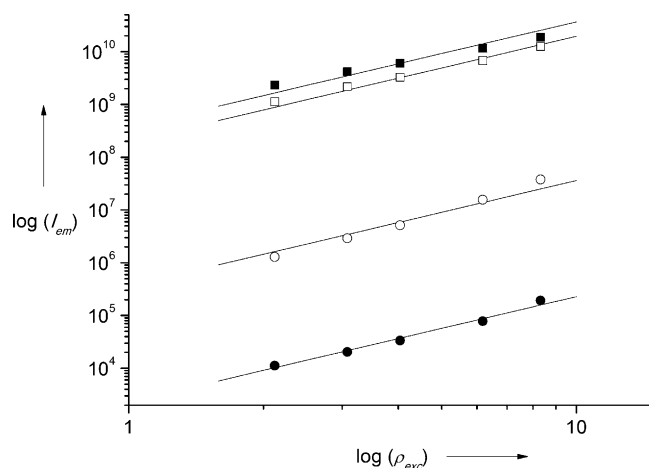


**Figure 4.** Double-logarithmic plots of the upconversion emission intensity (green and red emission) versus excitation density ( $\lambda_{\text{exc}} = 978$  nm) for different powder samples: (■) bulk  $\beta$ -NaYF<sub>4</sub>:Yb,Er, (□) bulk  $\beta$ -NaYF<sub>4</sub>:Yb,Er diluted with 3.5 times the amount of  $\beta$ -NaYF<sub>4</sub>, (○) 10 nm  $\beta$ -NaYF<sub>4</sub>:Yb,Er/ $\beta$ -NaYF<sub>4</sub> core/shell particles, (●) ca. 5 nm  $\beta$ -NaYF<sub>4</sub>:Yb,Er core particles. The slope of all lines is 2.

160 000 times weaker luminescence than the bulk material. The approximately 2 nm thick shell increases the upconversion efficiency of the particles by a factor of 160. Consequently, the ca. 10 nm core/shell particles are approximately 1000 times less efficient than the bulk material. The optically inactive NaYF<sub>4</sub> shell material, however, dilutes the system by a factor of 3.5 and therefore reduces the absorption of the excitation light. The figure shows that the same dilution of the bulk material with undoped NaYF<sub>4</sub> (see Figures S8 and S9) reduces the intensity of its upconversion emission by about a factor of 2. Taking this factor into account, the core/shell particles are still about 500 times less efficient than the bulk material. In fact, core/shell upconversion particles show in general a lower efficiency than the bulk material, even when the particles are larger than those reported here. Boyer et al., for instance, reported on 30 nm core/shell particles with an upconversion efficiency 10 times smaller than that of the bulk material.<sup>[19a]</sup> From a more general point of view, however, the low upconversion efficiency is somewhat surprising because core/shell nanocrystals of semiconductors and other down-conversion phosphors with comparable particle size show quantum yields above 50%.<sup>[20]</sup> It therefore appears possible to still increase the efficiency of upconversion particles by one to two orders of magnitude. This requires, however, that in future work the loss mechanisms are identified that strongly reduce the upconversion efficiency of  $\beta$ -NaYF<sub>4</sub>:Yb,Er nanocrystals.

## Acknowledgements

We thank Dr. K. Kömpe and H. Eickmeier for the TEM investigations and Dr. B. Herden and Prof. Dr. T. Jüstel for the solid-state synthesis of NaYF<sub>4</sub>:Yb(18%),Er(2%) powder phosphor.



**Keywords:** core/shell nanocrystals · lanthanides · luminescence · nanoparticles · upconversion

**How to cite:** *Angew. Chem. Int. Ed.* **2016**, 55, 1164–1167  
*Angew. Chem.* **2016**, 128, 1177–1181

- [1] D. Vennerberg, Z. Lin, *Sci. Adv. Mater.* **2011**, 3, 26–40.
- [2] a) S. F. Lim, R. Riehn, W. S. Ryu, N. Khanarian, C.-k. Tung, D. Tank, R. H. Austin, *Nano Lett.* **2006**, 6, 169–174; b) L. Wang, Y. Li, *Nano Lett.* **2006**, 6, 1645–1649; c) F. Wang, X. Liu, *Chem. Soc. Rev.* **2009**, 38, 976–989; d) J. Pichaandi, J.-C. Boyer, K. R. Delaney, F. C. J. M. van Veggel, *J. Phys. Chem. C* **2011**, 115, 19054–19064; e) H. Wen, H. Zhu, X. Chen, T. F. Hung, B. Wang, G. Zhu, S. F. Yu, F. Wang, *Angew. Chem. Int. Ed.* **2013**, 52, 13419–13423; *Angew. Chem.* **2013**, 125, 13661–13665.
- [3] a) P. Zhang, W. Steelant, M. Kumar, M. Scholfield, *J. Am. Chem. Soc.* **2007**, 129, 4526–4527; b) F. Wang, D. Banerjee, Y. Liu, X. Chen, X. Liu, *Analyst* **2010**, 135, 1839–1854; c) D. K. Chatterjee, M. K. Gnanasammandhan, Y. Zhang, *Small* **2010**, 6, 2781–2795.
- [4] a) A. Shalav, B. S. Richards, T. Trupke, K. W. Kramer, H. U. Güdel, *Appl. Phys. Lett.* **2005**, 86, 013505–013503; b) J. F. Suyver, A. Aebischer, D. Biner, P. Gerner, J. Grimm, S. Heer, K. W. Krämer, C. Reinhard, H. U. Güdel, *Opt. Mater.* **2005**, 27, 1111–1130; c) B. M. van der Ende, L. Aarts, A. Meijerink, *Phys. Chem. Chem. Phys.* **2009**, 11, 11081–11095.
- [5] C. Zhang, H.-P. Zhou, L.-Y. Liao, W. Feng, W. Sun, Z.-X. Li, C.-H. Xu, C.-J. Fang, L.-D. Sun, Y.-W. Zhang, C.-H. Yan, *Adv. Mater.* **2010**, 22, 633–637.
- [6] S. Baldelli, *Nat. Photonics* **2011**, 5, 75–76.
- [7] a) W. J. Kim, M. Nyk, P. N. Prasad, *Nanotechnology* **2009**, 20, 185301; b) T. Blumenthal, J. M. Meruga, P. S. May, J. J. Kellar, W. M. Cross, K. Ankireddy, S. Vunnam, Q. Luu, *Nanotechnology* **2012**, 23, 185305; c) J. M. Meruga, W. M. Cross, P. S. May, Q. Luu, G. A. Crawford, J. J. Kellar, *Nanotechnology* **2012**, 23, 395201; d) J. M. Meruga, A. Baride, W. Cross, J. J. Kellar, P. S. May, *J. Mater. Chem. C* **2014**, 2, 2221–2227.
- [8] a) N. J. J. Johnson, F. C. J. M. van Veggel, *Nano Res.* **2013**, 6, 547–561; b) G. Chen, H. Qiu, P. N. Prasad, X. Chen, *Chem. Rev.* **2014**, 114, 5161–5214.
- [9] a) J.-C. Boyer, F. Vetrone, L. A. Cuccia, J. A. Capobianco, *J. Am. Chem. Soc.* **2006**, 128, 7444–7445; b) H.-X. Mai, Y.-W. Zhang, R. Si, Z.-G. Yan, L.-D. Sun, L.-P. You, C.-H. Yan, *J. Am. Chem. Soc.* **2006**, 128, 6426–6436; c) G. S. Yi, G. M. Chow, *Adv. Funct. Mater.* **2006**, 16, 2324–2329; d) H.-X. Mai, Y.-W. Zhang, L.-D. Sun, C.-H. Yan, *J. Phys. Chem. C* **2007**, 111, 13721–13729; e) H.-X. Mai, Y.-W. Zhang, L.-D. Sun, C.-H. Yan, *J. Phys. Chem. C* **2007**, 111, 13730–13739; f) G.-S. Yi, G.-M. Chow, *Chem. Mater.* **2007**, 19, 341–343; g) Y. Sui, K. Tao, Q. Tian, K. Sun, *J. Phys. Chem. C* **2012**, 116, 1732–1739.
- [10] a) S. Heer, K. Kömpe, H. U. Güdel, M. Haase, *Adv. Mater.* **2004**, 16, 2102–2105; b) J. F. Suyver, J. Grimm, K. W. Krämer, H. U. Güdel, *J. Lumin.* **2005**, 114, 53–59; c) H.-S. Qian, Y. Zhang, *Langmuir* **2008**, 24, 12123–12125; d) Z. Li, Y. Zhang, *Nanotechnology* **2008**, 19, 345606; e) C. Liu, H. Wang, X. Li, D. Chen, *J. Mater. Chem.* **2009**, 19, 3546–3553.
- [11] a) A. D. Ostrowski, E. M. Chan, D. J. Gargas, E. M. Katz, G. Han, P. J. Schuck, D. J. Milliron, B. E. Cohen, *ACS Nano* **2012**, 6, 2686–2692; b) T. Rinkel, J. Nordmann, A. N. Raj, M. Haase, *Nanoscale* **2014**, 6, 14523–14530.
- [12] a) C. Li, Z. Quan, J. Yang, P. Yang, J. Lin, *Inorg. Chem.* **2007**, 46, 6329–6337; b) X. Liang, X. Wang, J. Zhuang, Q. Peng, Y. Li, *Adv. Funct. Mater.* **2007**, 17, 2757–2765; c) L. Wang, Y. Li, *Chem. Mater.* **2007**, 19, 727–734; d) F. Wang, X. Liu, *J. Am. Chem. Soc.* **2008**, 130, 5642–5643.
- [13] a) H. S. Choi, W. Liu, P. Misra, E. Tanaka, J. P. Zimmer, B. I. Ipe, M. G. Bawendi, J. V. Frangioni, *Nat. Biotechnol.* **2007**, 25, 1165–1170; b) M. Longmire, P. L. Choyke, H. Kobayashi, *Nanomedicine* **2008**, 3, 703–717.
- [14] A. N. Raj, T. Rinkel, M. Haase, *Chem. Mater.* **2014**, 26, 5689–5694.
- [15] a) N. J. J. Johnson, W. Oakden, G. J. Stanisz, R. S. Prosser, F. C. J. M. van Veggel, *Chem. Mater.* **2011**, 23, 3714–3722; b) B. Voß, J. Nordmann, A. Uhl, R. Kompan, M. Haase, *Nanoscale* **2013**, 5, 806–812.
- [16] a) F. Wang, Y. Han, C. S. Lim, Y. Lu, J. Wang, J. Xu, H. Chen, C. Zhang, M. Hong, X. Liu, *Nature* **2010**, 463, 1061–1065; b) D. J. Gargas, E. M. Chan, A. D. Ostrowski, S. Aloni, M. V. P. Altoe, E. S. Barnard, B. Sanii, J. J. Urban, D. J. Milliron, B. E. Cohen, P. J. Schuck, *Nat. Nanotechnol.* **2014**, 9, 300–305; c) F. Shi, Y. Zhao, *J. Mater. Chem. C* **2014**, 2, 2198–2203.
- [17] S. Dühnen, T. Rinkel, M. Haase, *Chem. Mater.* **2015**, 27, 4033–4039.
- [18] B. Voss, M. Haase, *ACS Nano* **2013**, 7, 11242–11254.
- [19] a) J.-C. Boyer, F. C. J. M. van Veggel, *Nanoscale* **2010**, 2, 1417–1419; b) N. J. J. Johnson, A. Korinek, C. Dong, F. C. J. M. van Veggel, *J. Am. Chem. Soc.* **2012**, 134, 11068–11071; c) D. J. Gargas, E. M. Chan, A. D. Ostrowski, S. Aloni, M. V. P. Altoe, E. S. Barnard, B. Sanii, J. J. Urban, D. J. Milliron, B. E. Cohen, P. J. Schuck, *Nat. Nanotechnol.* **2014**, 9, 300–305.
- [20] a) K. Kömpe, H. Borchert, J. Storz, A. Lobo, S. Adam, T. Möller, M. Haase, *Angew. Chem. Int. Ed.* **2003**, 42, 5513–5516; *Angew. Chem.* **2003**, 115, 5672–5675; b) D. V. Talapin, A. L. Rogach, A. Kornowski, M. Haase, H. Weller, *Nano Lett.* **2001**, 1, 207–211.

Received: September 21, 2015

Revised: October 20, 2015

Published online: December 3, 2015